Ion Flow Measurements in the Vicinity of Magnetic Islands in DIII-D

C.M. Samuell[1], J.D. Lore[2], M.W. Shafer[2], W.H. Meyer[1],S.L Allen[1], J. Howard[3]

[1] *Lawrence Livermore National Laboratory, Livermore, CA 94550, USA*

[2] *Oak Ridge National Laboratory, PO Box 2008, Oak Ridge, TN 37831, USA*

[3] *Australian National University, Canberra, ACT 0200, Australia*

Three-dimensional flows in the vicinity of magnetic islands have been imaged in the scrape off layer (SOL) for the first time in a tokamak. 3D flow measurements are essential to validate the numerical models used for developing island divertors for advanced stellarators like W7-X and to explain the resonant magnetic field (RMP) suppression of ELMs in future tokamak devices like ITER. In the case of island divertors, momentum loss from adjacent counter-streaming flows near magnetic islands can prevent access to the desired high-recycling regime [1, 2]. These flows have been observed experimentally in LHD [3] and HSX [1] and have been modeled extensively, along with 3D flows more generally, using the plasma fluid and kinetic neutral gas transport model EMC3-EIRENE [4, 1, 5, 6]. 2D and 3D measurements of the flow perturbation around magnetic islands has been achieved on DIII-D using Doppler Coherence Imaging measurements of C_2^+ impurity ions in the scrape off layer (SOL).

Coherence Imaging Flow Diagnostic

Flow velocity imaging is achieved in DIII-D using Doppler Coherence Imaging Spectroscopy (CIS) [7, 8]. This technique uses a heterodyne polarization interferometer to encode spectral information onto an image of visible emission. By using an interference filter, the emission can be isolated to a single ion species. Interferometric delay is produced by a birefringent crystal plate sandwiched between two linear polarizers. The delay depends on the crystal type, thickness, and

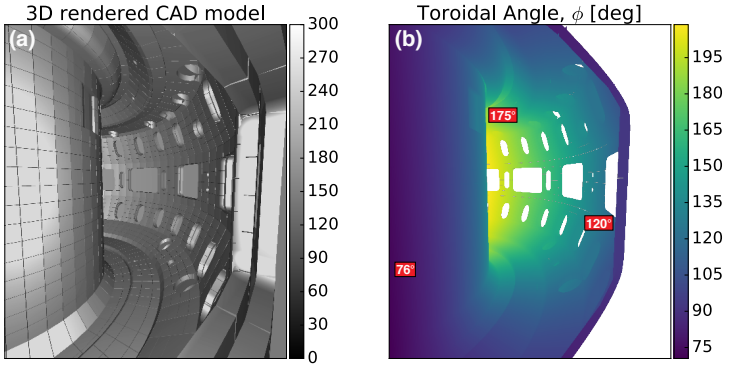

Figure 1: *(a) Rendering of the camera view and (b) the toroidal angle at the plasma facing surface throughout the camera view.*

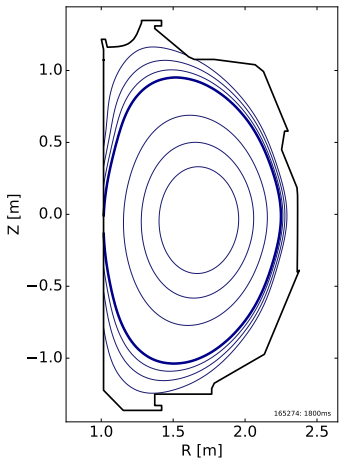

Figure 2: *EFIT equilibrium for the inner-wall limited L-mode discharge before application of the RMP.*

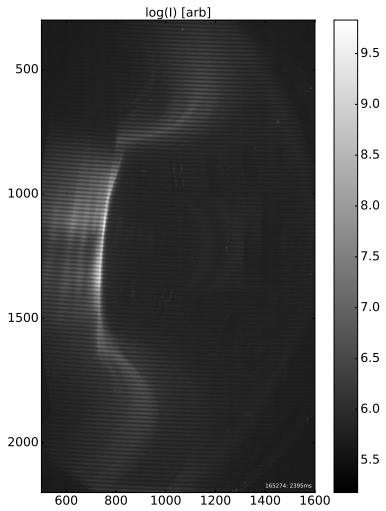

Figure 3: *CIS raw data of DIII-D inner wall limited L-mode plasma with n=1 applied RMP. Note the cropped axes.*

the plate's optical axis angle (cut angle). For measurements of the CIII multiplet at 465 nm, a 5.8 mm α-BBO crystal with a cut angle of 60° is used. This results in approximately 1400 waves of delay and was chosen to minimize the phase dependence on ion temperature [9]. The interferometer acts to superimpose a set of interference fringes onto the brightness image captured with a PCO.edge 5.5 2160x2560 pixel sCMOS camera. Interferogram phase is separated from the brightness using Fourier techniques and compared with an image of a quasi-monochromatic spectral source calculate the apparent Doppler velocity [9, 8].

A wide field of view system is employed on DIII-D to measure flows in the main chamber scrape off layer (SOL), as well as both upper and lower divertors. The view-port is located at a toroidal angle of 75° on the mid-plane with a view towards a 180°. This view is mostly tangential, however there are increasingly poloidal components of the view at both divertors.

A CAD rendering of the view is shown in Figure 1 alongside boundary values of the toroidal angle which varies between approximately 75 and 205 ° throughout the camera's view. Alignment of the camera image to the 3D CAD model is achieved using in-vessel fiducials during bright disruption events. The 3D model is then used in the tomographic inversion process and to account for spherical aberration introduced by the periscope viewing optics. The camera spatial resolution at the vessel boundary varies from about 0.2 mm/pixel to 4 mm/pixel. Both radial and vertical spatial resolutions are best in the near-field and mid-plane and are reduced in the relatively tightly spaced and sharply angled divertor regions. The spatial resolution of CIS velocity

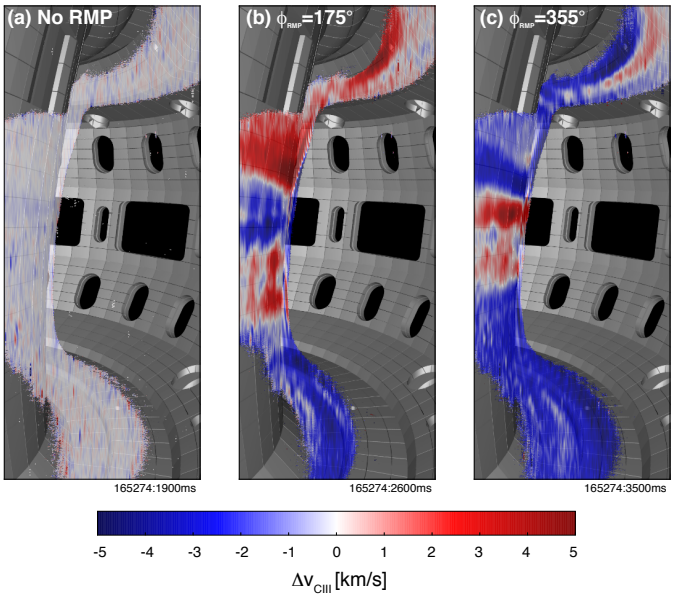

Figure 4: *Change in line-of-sight CIII velocity compared with an axisymmetric time slice. (a) Shows no difference when compared to another time where no RMP had been applied. (b) and (c) are two different n=1 applied RMP phases; poloidally varying acceleration and deceleration regions appear at different locations depending on the applied phasing.*

measurements is less than the camera resolution as the ability to resolve spatial features depends on the fringe frequency, the Fourier demodulation process, and the spatial scale of brightness features.

RMP island generation and ion acceleration

Magnetic islands were studied on DIII-D by applying a n=1 RMP to a L-mode inner-wall limited discharge. Steady-state axisymmetric plasmas were first established with B_T = -1.95 T (ion B×∇B down), I_P = 1.28 MA, and line averaged density of around 4×10^{19} m^{-3}. Approximately 4 MW of heating was applied consisting of 1 MW ohmic heating, 1.5 MW of injected neutral beam (NBI) power, and 1.5 MW of ECH injected into the core. Subsequently, RMP coils external to the machine (C-coils) were used to drive the n=1 resonant field (3.4 kAt peak) whose applied phase could be flipped and rotated through an entire 360° revolution. Adjusting the applied RMP phasing rotates the entire magnetic island chain through the camera's field of view to generate a three-dimensional picture of the plasma response.

Generation of magnetic islands was confirmed by measuring electron temperature profile flattening with Thomson scatting and Electron Cyclotron Emission (ECE) diagnostics. An EFIT equilibrium reconstruction of the discharge is shown in Figure 2. CIS camera data was acquired throughout each shot so that RMP-affected time slices could be compared to an axisymmetric plasma. An example of the raw CIS data is shown in Figure 3. Most of the CIII emission oc-

curs near the limiting surface, however emission extends out into the far scrape-off layer near the upper and lower divertors. CIII line-of-sight apparent velocities referenced to axisymmetric steady-state conditions are shown in Figure 4. For each time slice the apparent velocity image for a timeslice without RMPs was subtracted to directly measure the impact of inducing magnetic islands and to increase measurement accuracy. The emergence of large coherent island chains in the edge was correlated with the onset of localized changes in impurity ions velocity ($< \pm 10$ km/s). This pattern displayed a poloidal length scale of 30-40 cm along the inboard mid-plane and extended to the far-SOL ($\Psi_n > 1.1$). The polodial location of these pertubations changes as the applied RMP phase is changes and the magnetic islands rotate throughout the camera's field of view. Once established, changes in the RMP phase resulted in a localized velocity response that was faster than the camera's frame rate (50 Hz). Ongoing work is focusing on isolating the RMP and island contributions to flow perturbation and comparisons to EMC3-EIRENE modeling using recently developed synthetic diagnostic capability. This modeling will be used to separate competing contributions from ionization at the target plate, parallel pressure gradients, and the altered magnetic field line topology.

This work was supported in part under the auspices of the US Department of Energy under DE-FC02-04ER54698, DE-AC52-07NA27344 and DE-AC05-00OR22725. DIII-D data shown in this paper can be obtained in digital format by following the links at https://fusion.gat.com/global/D3D_DMP.

References

[1] A.R. Akerson et al., *Three-dimensional scrape off layer transport in the helically symmetric experiment HSX*, *Plasma Phys. Control. Fusion* **58** (2016) 084002

[2] Y. Feng, M. Kobayashi, T. Lunt and D. Reiter, *Comparison between stellarator and tokamak divertor transport*, *Plasma Phys. Control. Fusion* **53** (2011) 024099

[3] N. Ezumi, T. Kobayashi,N. Ohno, and K. Sawada, *Experimental observation of plasma flow alternation in the LHD stochastic magnetic boundary J. Plasma Fusion Res.* **8** (2011) 429-32

[4] Y. Feng et al., *Physics of island divertors as highlighted by the example of W7-AS*, *Nucl. Fusion* **46** (2006) 807-819

[5] F. Effenberg et al. *Numerical investigation of plasma edge transport and limiter heat fluxes in Wendelstein 7-X startup plasmas with EMC3-EIRENE*, *Nucl. Fusion* **57** (2017) 036021

[6] H. Frerichs et al. *The pattern of parallel edge plasma flows due to pressure gradients, recycling, and resonant magnetic perturbations in DIII-D*, *Physics of Plasmas* **22** (2015) 072508

[7] J. Howard et al., *Coherence Imaging of flows in the DIII-D divertor*, *Contrib. Plasma Phys* **51** No.2-3, (2011)

[8] C.M. Samuell, S.L. Allen, W.H. Meyer, J. Howard. *Absolute calibration of Doppler coherence imaging velocity images*, *Journal of Instrumentation* (2017) (submitted)

[9] J. Howard, C. Michael, F. Glass, and A. Danielsson *Time-resolved two-dimensional plasma spectroscopy using coherence-imaging techniques*, *Plasma Phys. Control. Fusion* **45** (2003) 1143-1166